Removal of REE and Th from solution by co-precipitation with Pb-phosphates

Julia Sordyl[1,2,*], Kacper Staszel[1], Mikołaj Leś[1], Maciej Manecki[1]

[1]Faculty of Geology, Geophysics and Environmental Protection, AGH University of Science and Technology, al. Mickiewicza 30, 30-059 Kraków, Poland

[2]Department of Earth Sciences, Uppsala University, Villavägen 16, SE-752 36 Uppsala, Sweden

*correspondence: sordyl@agh.edu.pl

Abstract

The supply of technologically important rare earth elements (REE) is a concern in Europe, hence the recovery of REE from alternative sources has recently become widely investigated. One of the problems is the lack of cost-effective technologies for REE recovery from leaching solutions. The present work investigated the potential for recovering REE and Th from leaching solutions by co-precipitation with Pb phosphates. A set of four experiments were conducted using analytical reagent grade chemicals to analyze the effects of Pb and different pH on the efficiency of REE and Th removal from aqueous solutions. After selecting the best conditions, two additional experiments were performed using solutions obtained from leaching REE-rich apatite mine waste.

The precipitates resulting from the experiments as well as the solutions before and after precipitation were analyzed. It was found that the formation of a crystalline mixture of REE- and Th- enriched pyromorphite, $Pb_5(PO_4)_3Cl$, and Pb-phosphates, about which little has been known so far, was responsible for complete (>99%) removal of REE and Th from aqueous solutions at pH 4 and 6. At lower pH, the removal is incomplete except for Sc and Th, which probably form a distinct phases. Besides that, no fractionation of LREE and HREE was observed. The experiments included the study of solutions resulting from the leaching of REE-rich apatite waste, which may contribute to the development of new technologies for REE recovery from wastes.

Keywords: rare earth elements, recovery, lanthanides, pyromorphite

1. Introduction

The rare earth elements are a group of chemically similar elements, including scandium (Sc), yttrium (Y), and 15 of the lanthanides: lanthanum (La), cerium (Ce), praseodymium (Pr), neodymium (Nd), promethium (Pm, synthetic element which does not exist in nature),

samarium (Sm), europium (Eu), gadolinium (Gd), terbium (Tb), dysprosium (Dy), holmium (Ho), erbium (Er), thulium (Tm), ytterbium (Yb), and lutetium (Lu). Thorium (Th), a radioactive element, although not classified as a REE, is very often found together with them and is worth considering jointly due to geochemical similarities. Lanthanides are subdivided into two subgroups: light rare earth elements (LREE) from La to Sm (REE with lower atomic numbers and masses, larger ionic radii) and heavy rare earth elements (HREE) from Eu to Lu (REE with higher atomic numbers and masses). Y is included in the HREE because of its geochemical associations with HREE in natural deposits (Henderson, 1984; Kumari et al., 2015; Peiravi et al., 2021). Sc is often not included in either of these groups due to its much smaller ionic radius. REE are widely used in traditional sectors including metallurgy, petroleum, textiles and agriculture, but thanks to their unique properties are increasingly critical to the high-technology, new materials, and low-carbon economy (Binnemans et al. 2013; Schulze and Buchert 2016; Dang et al., 2021; Gaustad et al. 2021; Silvestri et al. 2021). Due to their growing demand and risk of supply, the problem of REE availability has risen significantly over last years (Stone, 2009; McLellan et al. 2014; EU Report, 2020).

REE are usually recovered from various resources through hydrometallurgical processes consisting of leaching of the source material or concentrate, followed by extraction and separation of the elements from leached solutions through, for example, solvent extraction, ion-exchange, and precipitation (Verbaan et al., 2015; Tunsu et al., 2016; Sethurajan et al., 2019; Erust et al., 2022). Ion-adsorbed clays, as well as bastnasite, monazite, and xenotime, are the most frequently extracted rare earth natural (mineral) sources of REE (Jha et al., 2016; Vahidi et al., 2016; Alves et al., 2021). However, as China has monopolized the supply chain of REE and limits the export while the yearly demand of other countries is increasing, there has been a need to find new solutions to the limited supply. Circular economy approaches seem to be the most promising for this sector (Dang et al., 2021). As a result, there is a demand for intensive research into the recovery of REE from the large amount of waste produced in various industries. In most cases, exploration of new technologies for REE beneficiation from waste also includes hydrometallurgy (usually acid leaching) because downstream REE separation involves wet extraction and precipitation from solutions.

Recovery of valuable elements from secondary sources would include huge variety of material, e.g. fly, bottom, and incinerator ashes (Taggart et al., 2016; Liu et al., 2019);

industrial byproducts like slags, phosphogypsum or red mud (Kasina and Michalik, 2016; Yang et al., 2019; Salo et al., 2020; Das et al., 2021); electronic wastes (Ambaye et al., 2020; Dev et al., 2020; Ramprasad et al., 2022); phosphate rocks containing REE-rich apatite ($Ca_5[PO_4]_3(OH,F,Cl)$) (Pålsson et al., 2014; Battsengel et al., 2018; Wu et al., 2019; Peiravi et al., 2021); all of which being disposed in large quantities in landfills and tailings of mining waste rather than being recovered and reused (Du and Graedel, 2011; Zimmermann and Gößling-Reisemann, 2013). This is due to lack of technologies of REE recovery. Many research groups around the world are working to develop recycling processes using a number of different approaches. However, there are still many issues to be resolved for secondary sources to become actual REE sources.

Phosphate rocks containing REE-rich apatite, despite containing only trace amounts of REE, are promising due to their vast reserves (Wu et al., 2019). Many methods of REE recovery have been systematically studied, each with its own advantages and disadvantages. All such technology involves three main steps - (1) leaching, which depends on the mineral composition and quality of the concentrate, (2) recovery of REE from solution, and (3) further purification and separation stages. The first stage, leaching, is widely reported in the literature, tested and used in practice (e.g. Stone et al., 2016; Wu et al., 2018). The second step, however, the recovery of REE from the leaching solution, is found to be the most problematic. Colloidal slurry formation or the need for elevated temperatures are often a problem in this kind of ore and waste processing. Currently known methods for recovering REE from solutions originated from acid decomposition of raw material involve precipitation, crystallization, ion exchange or solvent extraction. These are promising approaches that have the potential to remove REE and Th from solution and to produce a marketable REE end product, free of impurities. However, these applications vary in terms of effectiveness or cost (for discussion see Pereao et al., 2018; Wu et al., 2018; Peiravi et al., 2021).

This work explores for the first time the process of recovering REE and Th from leaching solutions by co-precipitation with Pb phosphates. The proposed solution takes advantage of their very low solubilities. These processes occur with very high yields already at ambient temperatures for both LREE and HREE. The formation of crystalline pyromorphite, $Pb_5(PO_4)_3Cl$, containing REE (and contributing to the complete removal of Pb from the final solutions) is accompanied by the co-precipitation of Pb-REE phosphates, about which little has been known

so far. The experiments included the study of solutions resulting from the leaching of actual waste apatite-REE, which will contribute to the development of future new technologies for the beneficiation of REE from wastes.

2. Materials and methods

To determine the effect of the presence of Pb on the formation of REE and Th phosphates from aqueous solutions, three sets of experiments were conducted: precipitation of REE and Th phosphates in the absence of Pb (control experiment '0'), precipitation of REE and Th phosphates in the presence of Pb (experiments A, B, and C), and precipitation of REE and Th phosphates from solutions resulting from acid leaching of apatite from mine waste (experiments D and E). All compounds were precipitated under ambient conditions by a dropwise addition of solutions. The composition and concentrations in each solution varied between experiments (Table 1, *solution I* was added to *solution II*). All initial solutions containing REE and Th were sampled and analyzed using Inductively Coupled Plasma-Optical Emission Spectrometry (ICP-OES) and the concentrations are referred to as "before experiment". In the experiments A, B, and C, the molar ratio of Pb:REE equaled to 4:1, 1:1, and 1:4, respectively, and each experiment was repeated at pH 2, 4, and 6. The pH was maintained using 1M HNO_3 (POCH, purity ≥ 99.9%) and 1M NaOH (POCH, purity ≥ 99.9%) using an ELMETRON CPI 501 m and glass electrode (Elmetron Sp.j., Zabrze, Poland). Experiments A-C and '0' were conducted using analytical reagent grade chemicals dissolved in a double-distilled water: $Pb(NO_3)_2$ (Chempur, purity ≥ 99.9%), $NaH_2PO_4{\cdot}H_2O$ (Chempur, purity ≥ 99.9%), NaCl (Eurochem, purity ≥ 99.9%), and MISA Standard 5: Ce, Dy, Er, Eu, Gd, Ho, La, Lu, Nd, Pr, Sc, Sm, Tb, Th, Tm, Y, Yb @ 100 µg/mL in 2% HNO_3 (REE without promethium (Pm); VHG, purity ≥ 99.9%). For the experiments D (with HCl, Chempur, purity ≥ 99.9%) and E (with H_3PO_4, Chempur, purity ≥ 99.9%), solutions obtained by leaching of REE-rich apatite ($Ca_5(PO_4)_3(F,OH)$ containing 2 wt% of REE_2O_3) waste from iron mine was used. The details of leaching procedure are not provided here, as it was not the objective of this paper. Briefly, in first step of experiment D, a 1M HCl was used for leaching at ambient temperature for 72 hours (solid-liquid ratio equal to 1g:2ml). In the second step, the solid waste was separated from the leaching solution, and new solution containing $Pb(NO_3)_2$ and $(NH_4)_2HPO_4$ was dropwise mixed with the leaching solution (containing Cl, REE and Th, among others; Pb excess in relation to REE). In the first step of experiment E, a 7M H_3PO_4 was used for leaching at ambient temperature for 48 hours (solid-liquid-solid ratio equal to 1g:10ml). In the second step, the

solid waste was separated from the leaching solution, and new solution containing $Pb(NO_3)_2$ and NaCl was dropwise mixed with the leaching solution (containing PO_4, REE and Th, among others; Pb excess in relation to REE). The pH was maintained at between 3 and 4 with 1M NaOH. After experiments, the precipitates were separated from solutions by centrifugation (5000 rpm, centrifugal force 2520 x g, 3 minutes), washed with double-distilled water, air-dried and analyzed using powder X-ray diffraction (XRD) and scanning electron microscope equipped with an energy dispersive analyzer (SEM-EDS). The solutions (referred to as "after experiment") were analyzed using ICP-OES.

Table 1. Composition of initial solutions used for the experiments.

	Solution I	*Solution II*
Exp. '0'	3.25 mmol REE+Th/L	20 mmol PO_4/L and 3.3 mmol Cl/L
Exp. A	13 mmol Pb/L and 3.25 mmol REE+Th/L	20 mmol PO_4/L and 3.3 mmol Cl/L
Exp. B	3.25 mmol Pb/L and 3.25 mmol REE+Th/L	20 mmol PO_4/L and 3.3 mmol Cl/L
Exp. C	3.25 mmol Pb/L and 13 mmol REE+Th/L	20 mmol PO_4/L and 3.3 mmol Cl/L
Exp. D (with HCl)	1.3 mmol REE+Th/L in 1M HCl *	20 mmol PO_4/L and 13 mmol Pb/L
Exp. E (with H_3PO_4)	0.8 mmol REE+Th/L in 7M H_3PO_4 *	13 mmol Pb/L and 3.3 mmol Cl/L

* solutions obtained by leaching of REE-rich apatite waste

Phase composition of the precipitates after the experiments was determined using XRD. Conventional powder diffraction patterns were recorded using a Rigaku SmartLab diffractometer (Neu-Isenburg, Tokyo, Japan) with monochromatized CuKα radiation, in the range of 2 – 75° 2θ with a step size of 0.05° and a counting time of 1s/step. Phase identification of the solids was performed using XRAYAN (Marciniak et al., 2006) and the International Centre for Diffraction Data (ICDD) powder diffraction pattern database.

For imaging and semi-quantitative analyses of the precipitates, powders mounted on conductive carbon tapes were investigated using a FEI QUANTA FEG 200 SEM-EDS (Thermo Fisher Scientific, Waltham, MA, USA) operated at accelerating voltage of 15 kV. The samples were imaged and analyzed at low vacuum with no conductive coating applied. EDS spot analysis was performed on isolated larger grains as well as homogeneous aggregates of smaller grains.

REE, Th, and Pb concentrations in solutions before and after the precipitation experiments were analyzed at the AGH-UST Hydrogeochemical Laboratory using the ICP-OES technique (Optima 7300 DV spectrometer from Perkin Elmer™). The multi- and single element standard

solutions of Sigma Aldrich® were used for preparation of the calibration curve. Detection limits and measurements uncertainties for all analyzed elements are presented in Table 2. Two different uncertainties are shown: U [%] (k=2.95%) for D.L. represents measurement uncertainties for concentrations at the detection limit, while the second column named U [%] (k=2.95%) represents measurement uncertainties for higher concentrations.

Table 2. Detection limits (D.L.) and measurement uncertainties (U) with a coverage factor (k) of elemental concentrations in solutions analyzed with ICP-OES.

	D.L. [mg/L]	U [%] (k=2.95%) for D.L.	U [%] (k=2.95%)
Sc	0.01	17.44	6.81
Y	0.01	12.49	4.54
La	0.01	10.21	4.5
Ce	0.01	45.27	12.54
Pr	0.01	26.27	3.9
Nd	0.01	32.52	5.56
Sm	0.01	16.54	6.07
Eu	0.01	15.24	7.06
Gd	0.01	18.42	3.55
Tb	0.01	19.95	5.77
Dy	0.01	15.98	6.63
Ho	0.01	14.89	5.34
Er	0.01	30.68	6.31
Tm	0.01	10.16	4.11
Yb	0.01	12.77	5.28
Lu	0.01	14.52	4.53
Th	0.01	44.35	6.22
Pb	0.01	23.92	6.23

3. Results and discussion

3.1. Precipitation of REE and Th phosphates in the absence of Pb

The experiments described in this section were carried out to precipitate REE phosphates according to equation (1):

$$REE^{3+} + PO_4^{3-} + nH_2O = REEPO_4 \cdot nH_2O \quad (1)$$

Since the REE solution was acidic (pH < 1), NaOH was used to raise the pH, similar to the experiments described in the literature. REE phosphate precipitation methods with neutralization using NaOH or ammonia are reported as a potential way to recover REE from phosphoric acid solutions (e.g., Habashi, 1985; Zakharova et al., 1996). According to a review

paper by Wu et al. 2018, the precipitation method using ammonia or NaOH neutralization to pH = 2 – 3 produces a colloidal precipitate of rare earth phosphates. It is a simple process with relatively high REE recovery (> 90%). However, they pointed to the high consumption of reagents and low purity of REE as the main challenges, which make the method uneconomical for industrial application.

Our goal was to control the fractionation of REE from solutions and the effect of pH on removal. These experiments served as control experiments for co-precipitation of REE phosphates in the presence of Pb at the very same precisely controlled laboratory conditions. Comparison of the results of experiments at pH 2, 4, and 6 indicates an increase of the removal efficiency with pH (Table 3). At the lowest pH, the average removability for all REE was 51% (σ = 6.17%). No significant differences were noted for LREE and HREE, which ranged from 49(±6)% to 51(±12)% and from 46(±6)% to 50(±7)%, respectively, indicating no fractionation. Surprisingly, however, Sc and Th showed much higher removal rate, reaching 75(±3)% and 99% (Figure 1). In contrast, the experiments at pH 4 and 6 proved to be highly effective for removal of both REE and Th removal (at the rate of over 99%).

Table 3. Elements concentrations [mg/L] in the solutions before and after precipitation and the percentage of removal in the control experiments (exp. '0') in various pH (2, 4, 6). Measurement uncertainties (±) are given only if they are greater than a significant value.

Element	pH = 2			pH = 4			pH = 6		
	Before [mg/L]	After [mg/L]	Removal rate [%]	Before [mg/L]	After [mg/L]	Removal rate [%]	Before [mg/L]	After [mg/L]	Removal rate [%]
Sc	23.89 ± 1.63	5.98 ± 0.41	75 ± 3	24.38 ± 1.66	0.02	99	23.90 ± 1.63	b.d.	>99
Y	23.81 ± 1.08	11.96 ± 0.54	50 ± 5	24.34 ± 1.11	b.d.	>99	23.85 ± 1.08	b.d.	>99
La	23.40 ± 1.05	11.66 ± 0.52	50 ± 4	23.87 ± 1.07	b.d.	>99	23.41 ± 1.05	b.d.	>99
Ce	21.92 ± 2.75	10.31 ± 1.29	51 ± 12	21.96 ± 2.75	b.d.	>99	21.37 ± 2.68	b.d.	>99
Pr	23.32 ± 0.91	11.68 ± 0.46	50 ± 4	23.83 ± 0.93	b.d.	>99	23.26 ± 0.91	b.d.	>99
Nd	23.13 ± 1.29	11.40 ± 0.63	50 ± 5	23.34 ± 1.30	b.d.	>99	22.81 ± 1.27	b.d.	>99
Sm	23.28 ± 1.41	11.70 ± 0.71	49 ± 6	23.84 ± 1.45	0.07	99	23.35 ± 1.42	0.05	99
Eu	23.11 ± 1.63	11.58 ± 0.82	49 ± 7	23.49 ± 1.66	b.d.	>99	23.05 ± 1.63	b.d.	>99
Gd	23.90 ± 0.85	12.02 ± 0.43	50 ± 4	24.42 ± 0.87	0.17 ± 0.01	99	23.84 ± 0.85	0.18 ± 0.01	99
Tb	23.69 ± 1.37	12.66 ± 0.73	46 ± 6	24.17 ± 1.40	b.d.	>99	23.65 ± 1.37	0.03	99
Dy	23.43 ± 1.55	11.68 ± 0.77	50 ± 7	23.87 ± 1.58	b.d.	>99	23.43 ± 1.55	b.d.	>99
Ho	23.34 ± 1.25	11.63 ± 0.62	50 ± 5	23.80 ± 1.27	b.d.	>99	23.34 ± 1.25	b.d.	>99
Er	23.55 ± 1.48	11.81 ± 0.74	49 ± 6	23.86 ± 1.50	0.06	99	23.44 ± 1.48	0.04	99
Tm	23.67 ± 0.97	11.94 ± 0.49	49 ± 4	24.23 ± 1.00	0.02	99	23.77 ± 0.98	b.d.	>99
Yb	23.62 ± 1.25	11.88 ± 0.63	49 ± 5	24.12 ± 1.27	b.d.	>99	23.66 ± 1.25	b.d.	>99
Lu	24.11 ± 1.09	12.05 ± 0.55	50 ± 5	24.66 ± 1.12	0.02	99	24.18 ± 1.10	b.d.	>99
Th	23.81 ± 1.48	0.34 ± 0.02	99	24.46 ± 1.52	0.14 ± 0.01	99	24.01 ± 1.49	0.28 ± 0.02	99

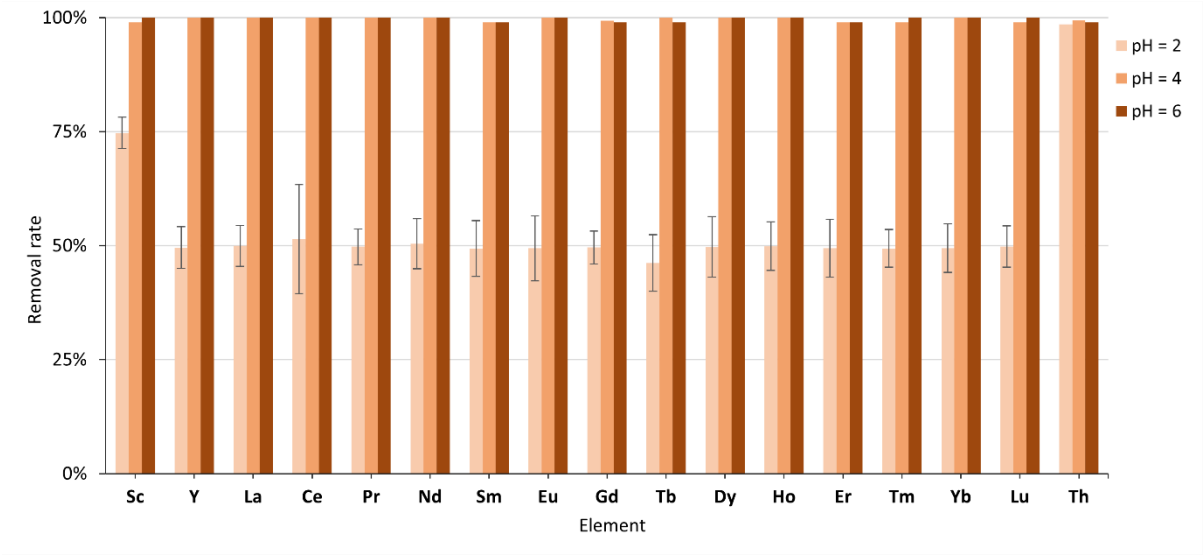

Figure 1. Variations of REE and Th removal rate [%] from solutions by phosphate precipitation depending on pH (exp. '0').

At all three experiments the elements were removed from solutions by precipitation. For the experiment at pH = 2, only turbidity of the solution was observed, suggesting the precipitation of an extremely fine precipitate, the amount of which, when recovered by centrifugation, proved impossible to analyze. At pH 4 and 6 more precipitate was formed, which very slowly settled on the bottom (1 hour of complete stagnation for the tested volumes) and the solution above it remained cloudy anyway. The solutions and solids were then separated by centrifugation to allow further characterization. The diffraction curves indicated poor crystallinity and were challenging for identification (Figure 2). The pattern somewhat resembled rhabdophane-La ($LaPO_4 \cdot 0.6H_2O$; ICDD-PDF 46-1439), although it did not allow unambiguous identification. This is probably due to the fact that the precipitate was a mixture of weakly crystallized phosphates of various REE and Th, not all of which adopt the structure of rhabdophane. In the backscattered electron images (BSE) the agglomerates of very fine precipitate were apparent, from which the morphology of the single crystals could not be read (Figure 3). It is in line with the results obtained by Wu et al. (2019) that REE phosphates obtained at the temperature in the range 25 – 60˚C are amorphous and hydrated, and the degree of hydration decreases as the temperature is raised.

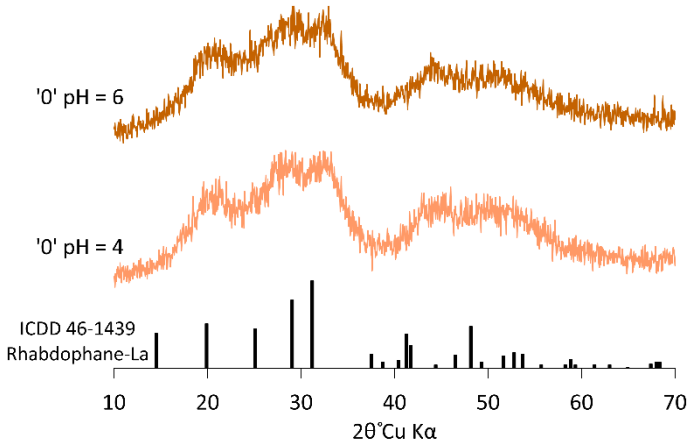

Figure 2. XRD patterns of poorly crystalline precipitates resulting from precipitation of REE and Th phosphates in the absence of Pb at pH = 4 and 6 (exp. '0').

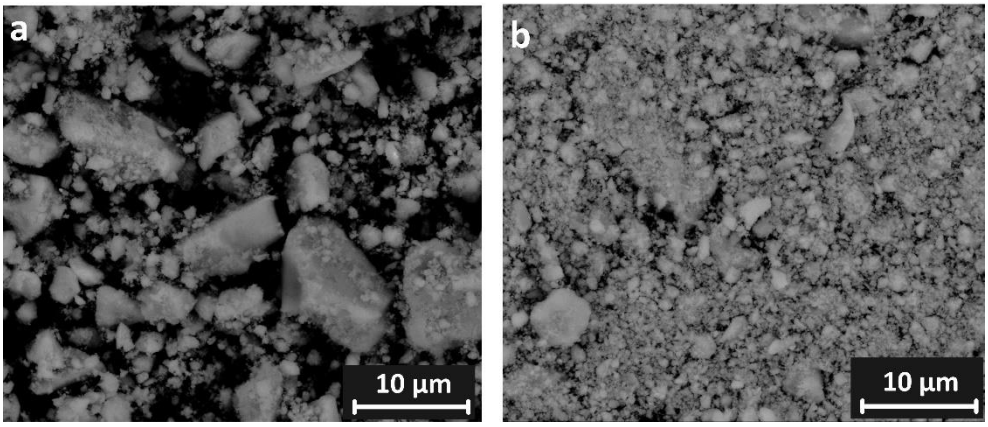

Figure 3. Backscattered electron images of agglomerated precipitates of REE and Th-phosphates from experiment '0': a) at pH = 4, and b) at pH = 6.

In summary, the precipitation of REE and Th phosphates from solutions at ambient temperature strongly depends on pH. Under the conditions tested, it was not very effective at pH = 2 and the solids were hard to recover. At pH = 4 and 6 the removal rate was above 99% and the precipitation was faster than at pH = 2 and the process is extremely efficient from the perspective of removability of all REE and Th. However, the process is relatively fast at the laboratory scale, i.e., it takes no more than 1 hour for the fine precipitate to settle to the bottom of the beaker completely, this could prove to be a long process when transferred to a larger scale. Therefore, the same conditions were used for further experiments, but with one

change: the addition of lead, which, according to the hypothesis, will affect the crystallinity of the resulting precipitate, allowing easy separation from the solution, thereby not reducing the high degree of removal of valuable elements from the solution.

3.2. Precipitation of REE and Th phosphates in the presence of Pb

REE and Th precipitation experiments in the presence of Pb were carried out at three different Pb:REE molar proportions (1:4; 1:1; 4:1, experiments A, B, and C respectively), each at three different pHs (2, 4, and 6) to control the effect of Pb content and acidity on the effectiveness of REE removal. The element concentrations in the solutions before and after precipitation are presented in Table S1 (Supplementary materials) while the removal rates [%] are compared in Table 4.

Similarly to the control experiment '0', there is a significant difference of REE removal rate between the experiments conducted at the lowest pH = 2 and experiments at pH = 4 and 6, but the Pb:REE ratio also played the role. At pH = 2, the REE were removed at the level of 53(±4)% – 59(±5)%, 61(±4)% – 84(±1)%, and 47(±6)% – 53(±6)% for the experiment A, B, and C, respectively. In contrast, Sc and Th were almost completely removed (Sc: 96(±1)% and Th: 99(±1)%). The best efficiency was observed for the experiment B (Pb:REE = 1:1) as presented in Figure 4. For the pH = 4 and 6, REE were almost completely removed from the solutions (98% – >99%) for all investigated Pb:REE proportions.

A similar trend was observed for the removal of Pb. At pH = 2, a significant amount of Pb still remained in solution (concentrations between 305.17(±19.01) mg/L and 190.9(±11.9) mg/L, Table S1). This indicates that pH = 2 is too low for complete precipitation of Pb and REE phosphates from aqueous solutions. Pb removal at the level of 99 – >99% was reached at pH = 4 and 6.

Table 4. Removal rate [%] of elements from the solutions after precipitation in the presence of Pb (exp. A, B, C) at various pH (2, 4, 6). Uncertainties (±) are given only if they are ≥ 1%. Elemental concentrations are provided in Table S1.

Element	A			B			C		
	2*	4	6	2	4	6	2	4	6
	Removal rate [%]								
Sc	96 ± 1	99	99	97	>99	>99	97	99	99

Y	53 ± 4	99	>99	61 ± 4	>99	>99	48 ± 5	>99	>99
La	55 ± 4	99	>99	70 ± 3	>99	>99	49 ± 5	99	>99
Ce	58 ± 10	>99	>99	74 ± 6	>99	>99	51 ± 12	>99	>99
Pr	57 ± 3	99	>99	84 ± 1	>99	>99	52 ± 4	>99	>99
Nd	58 ± 5	98	>99	83 ± 2	>99	>99	53 ± 5	>99	>99
Sm	59 ± 5	99	99	83 ± 2	>99	>99	53 ± 6	>99	>99
Eu	58 ± 6	99	>99	82 ± 3	>99	>99	52 ± 7	>99	>99
Gd	56 ± 3	98	99	75 ± 2	99	99	50 ± 4	99	99
Tb	54 ± 5	99	>99	76 ± 3	>99	>99	47 ± 6	>99	>99
Dy	56 ± 6	99	>99	73 ± 4	>99	>99	50 ± 7	>99	>99
Ho	55 ± 5	99	>99	70 ± 3	>99	>99	49 ± 5	>99	>99
Er	54 ± 6	99	99	68 ± 4	99	99	49 ± 6	99	99
Tm	55 ± 4	99	98	69 ± 3	>99	>99	49 ± 4	>99	>99
Yb	56 ± 5	99	>99	69 ± 3	99	>99	50 ± 5	99	>99
Lu	56 ± 4	99	>99	67 ± 3	>99	>99	49 ± 5	99	>99
Th	99	98	98	>99	99	99	99	99	99
Pb	88 ± 1	99	>99	71 ± 4	99	>99	56 ± 6	99	>99

* pH

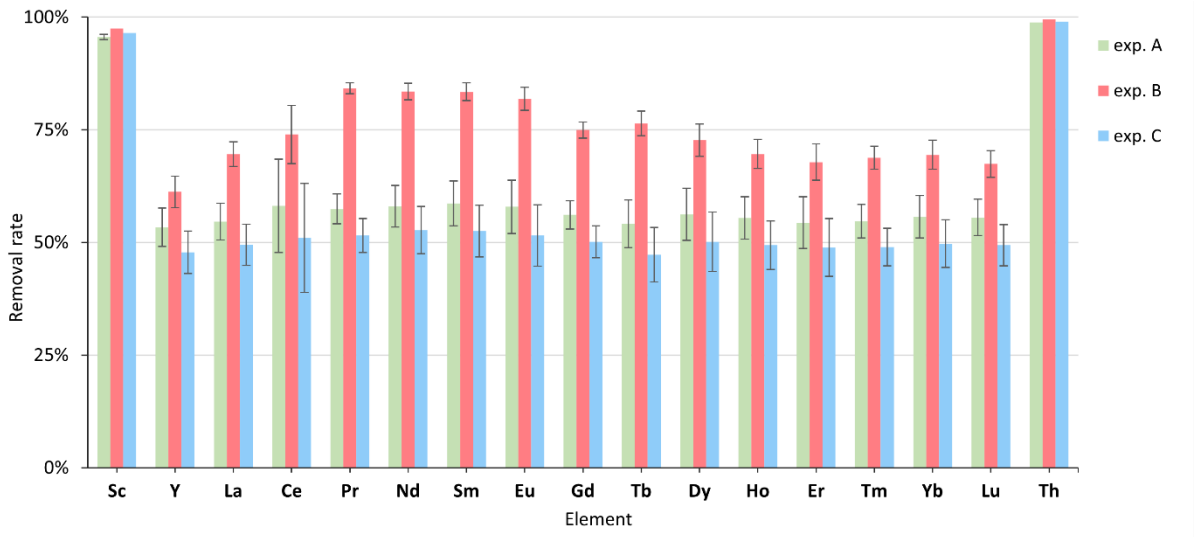

Figure 4. Variation of REE and Th removal rate [%] from solutions at pH = 2 by precipitation of phosphates in the presence of Pb depending on Pb:REE molar ratio: A = 1:4, B = 1:1, and C = 4:1.

The diffraction patterns of the precipitates are presented in Figures 5 – 7. At the highest Pb content (Pb:REE = 4:1), the reaction product was crystalline analog of pyromorphite (Figure 5). Slightly elevated background around 19˚ and 29˚ 2θ is apparent in the diffraction curves of the products obtained at pH = 4 and 6. This may indicate a slight admixture of another, poorly crystalline phase. No such additional peaks were observed for the phase precipitated at pH =

2. It is therefore possible that the precipitation of this additional phase is responsible for the greater removal of REE from solutions at pH = 4 and 6.

A similar difference in the XRD patterns of the precipitates resulting from the experiments at pH = 2 and those at pH = 4 and 6 was noted for experiments B (Pb:REE = 1:1). The products formed at pH = 2 were more crystalline than those obtained at higher pH. The main component of the precipitates was pyromorphite (Fig. 6). At higher pH, it was accompanied by a small amount of another, yet unidentified phase, whose weak but sharp and distinct reflections were apparent at 19.98; 28.48; 37.51; 41.36 °2θ, similar to phases described by Staszel et al. (submitted). In this case, the increase in REE removability from solutions at higher pH was also correlated with the appearance of new diffraction peaks. The absence of a diffraction peak around 14 °2θ suggested that this is probably not a phase resembling rhabdophane.

The precipitates formed at Pb:REE ratio equal to 1:4 (experiment C) were very poorly crystallized. The diffraction patterns were almost identical for the products obtained at all pH conditions used in the experiments (Figure 7). The positions of the reflections did not correspond to pyromorphite. The diffraction pattern somewhat resembled the one for the rhabdophane, but differences in the positions of the strongest reflections and the absence of a characteristic peak at 14 °2θ indicated that this is probably a different, new phase representing a Pb-REE phosphate.

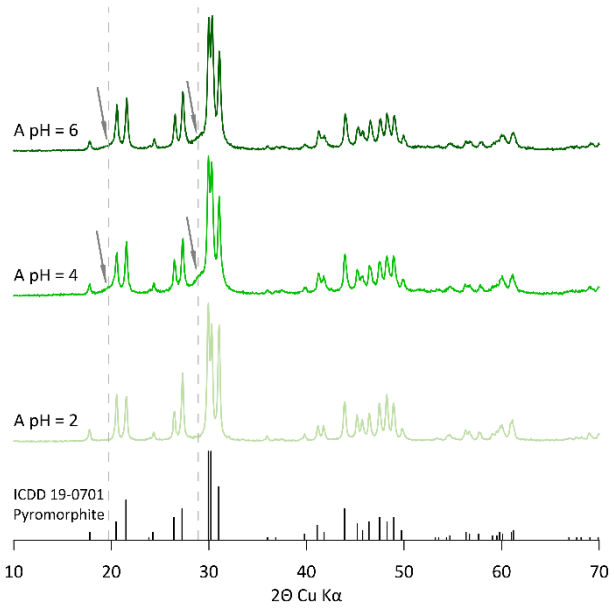

Figure 5. Diffraction patterns of pyromorphite precipitated in Experiment A at different pH. Arrows indicate small admixtures of additional, poorly crystalline phases, which are absent at pH=2.

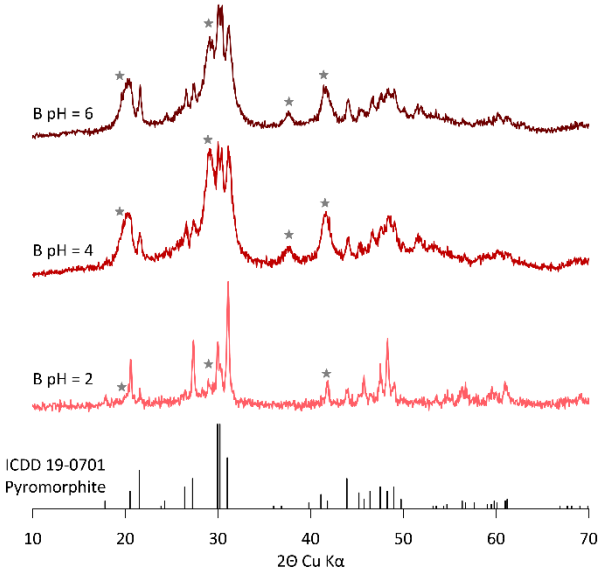

Figure 6. Diffraction patterns of phosphate precipitates resulting from experiment B at different pH. Pyromorphite was accompanied by another phase (marked with asterix), which was more crystalline at pH = 2 and more abundant at higher pH.

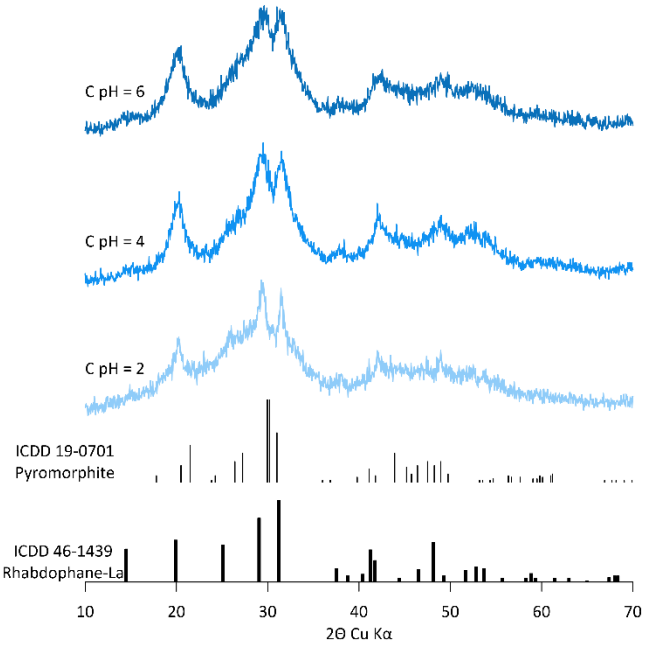

Figure 7. Diffraction patterns of poorly crystalline precipitates resulting from experiment C at different pH.

Observations of BSE images are in line with the XRD results. Due to the fine crystallinity of phases, and the fact that the aggregates always contained a mixture of both phases, the detailed characterization of chemical composition was hard to conduct. However, a semi-quantitative EDS analysis was performed to distinguish changes in the weight proportions of the key elements. These results, although normalized to total of 100% and of too poor quality to determine the chemical formulas of the resulting phases, accurately reflected other observations and are therefore presented and discussed here. We compare EDS spectra of two distinct phases for each experimental series (A, B, C) and do not differentiate between the pH conditions, as no differences were noted within the series.

BSE images of precipitates from experiment A revealed the presence of at least two different phases (Figure 8). More crystalline phase with significantly larger and well formed crystals was pyromorphite (as indicated by the presence of Cl) while the accompanied phase, indicated also by XRD (Figure 5) remained unidentified. Pyromorphite contained less lanthanides than the other phase (Figure 9.A1 and Figure 9.A2). However, no significant differences between Y, Sc, and Th content were observed.

BSE images of B series precipitates (Figure 8) revealed significant changes in morphology and proportion of two phases, not just between different pH conditions in this series, but also in comparison to series A. At pH = 2, at least two phases were present: bright, elongated needles (probably pyromorphite as indicated by the presence of Cl) associated with significant amounts of a second phase that formed shapeless aggregates. As pH increased, the presence of visible, well-formed pyromorphite crystals decreased to the point that only small needles, less than 5 µm in length were seen poking through the dominant, unidentified phase. This trend was similar to that observed in the XRD patterns (Figure 6). EDS revealed significant differences in elemental proportions between two phases. Pyromorphite seemed to incorporate 10.2 wt% of lanthanides, < 1 wt% of Th and Sc, and 1.1 wt% of Y (Figure 9.B1). The second phase, with much lower Pb content and higher P content compared to pyromorphite, incorporated 23.11 wt% of lanthanides, 6.7 wt% of Th and Sc, and 1.7 wt% of Y (Figure 9.B2). The observations of BSE images of precipitates formed at C series proved the absence of pyromorphite (Figure 8). The products were identical for all pH conditions used in the experiments. Only aggregates of poorly crystalline phase were apparent. Even though

pyromorphite was not present, aggregates of two distinct phases could be distinguished with BSE contrast and elemental composition. Both phases contained similar amounts of Pb and P but differed significantly in REE and Th content: one phase was clearly enriched in lanthanides (35.43 wt%) and Y (3.17 wt%), thus depleted in Th and Sc (1.55 and 1.97 wt%). The second phase, slightly less rich in lanthanides and Y, though still at nearly 20 and 1.93 wt%, respectively, instead was clearly enriched in Th and Sc (9.78 and 9.51 wt%).

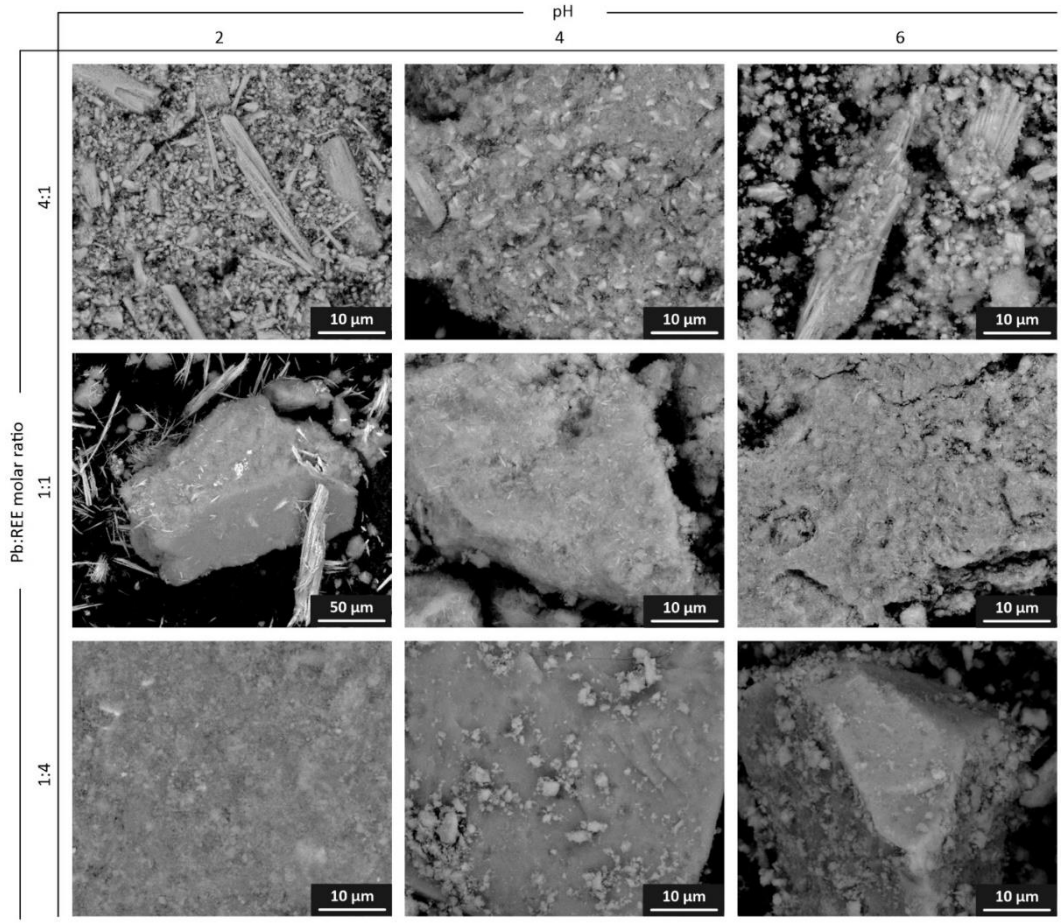

Figure 8. Backscattered electron images of precipitates obtained at various Pb:REE molar proportions and pH.

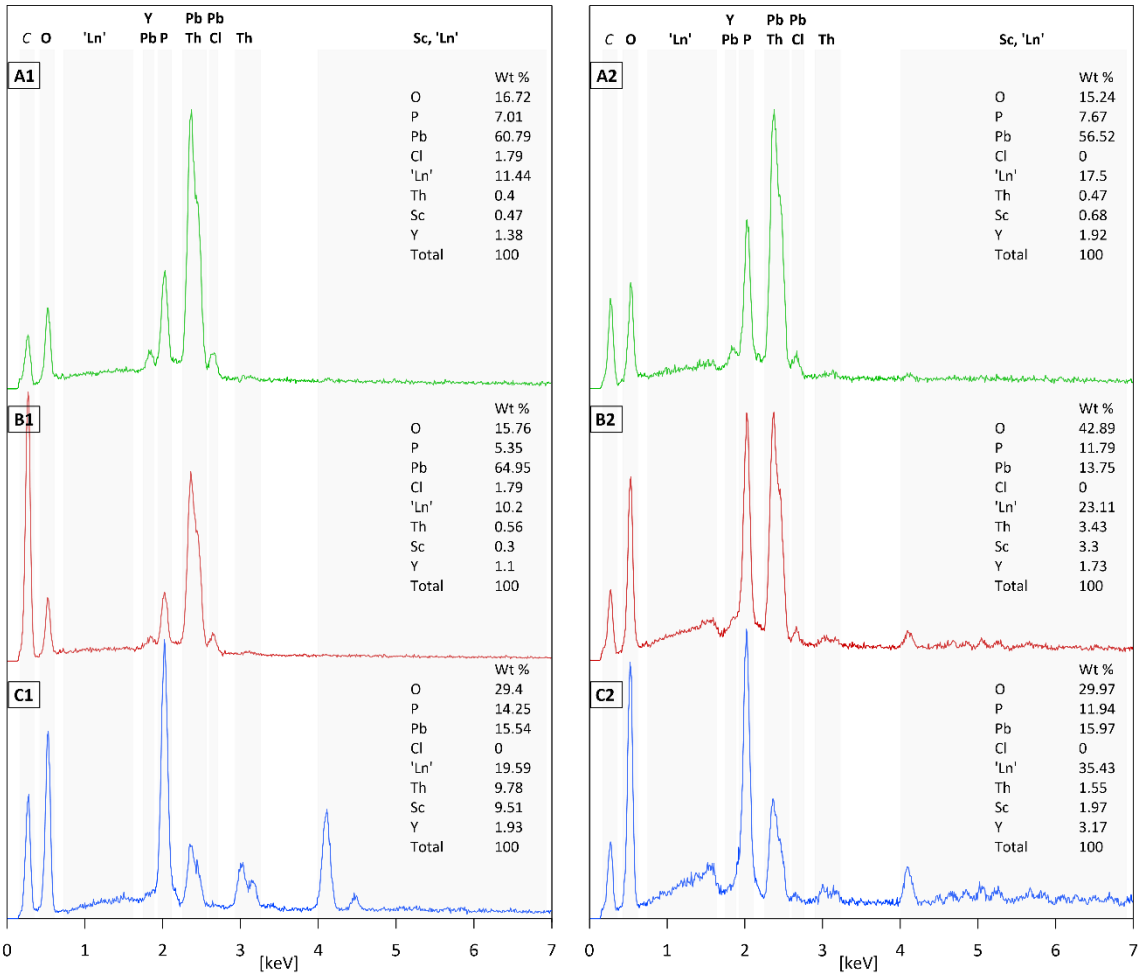

Figure 9. EDS spectra along with semi-quantitative spot analyses [wt%, normalized to 100%] of precipitates obtained at various Pb:REE molar ratios: A1 and A2 represent the two distinct phases detected in experiment A; B1 and B2 represent the two distinct phases detected in experiment B; C1 and C2 represent the two distinct phases detected in experiment C. 'Ln' stands for all lanthanides (a sum for the elements from La to Lu). A first peak at ca. 0.28 keV comes from carbon mounting tape.

In summary, no significant differences in the efficiency of REE removal by precipitation of phosphates from aqueous solutions were observed between the experiments in the absence and in the presence of Pb. However, a difference occurs in the precipitates' characteristics and physical properties. pH = 2 is too low for efficient Pb-REE phosphate precipitation but no REE fractionation was observed, with both LREE and HREE precipitating at the same level. However, Sc and Th are removed from the solution at much higher rates. At pH = 4 and 6 complete removal of REE, Th and Pb is observed. At the conditions tested, a mixture of at least

two phases precipitates which show a different degree of incorporation of REE and Th. Pyromorphite incorporates up to 13.4 wt% of REE, which probably occurs through the following reaction (Pan and Fleet, 2002; Sordyl et al., 2023):

$REE^{3+} + Na^{+} <=> 2Pb^{2+}$ (2)

The second phase, which incorporates REE at the level of up to 40.5 wt%, is yet poorly characterized Pb-REE phosphate, which is not an analog of any known mineral.

3.3. Precipitation of REE and Th phosphates from solutions resulting from leaching of apatite

To verify the high efficiency of the REE and Th removal from solutions by the desired method in other media, we conducted two experiments using the solutions obtained after leaching from rocks containing REE and Th minerals. The first experiment was conducted in 1M HCl, while the second in 7M H_3PO_4, both containing different initial concentrations of REE and Th (Table 5). For the experiment in HCl, solution containing Pb^{2+} and PO_4^{3-} was added by dropwise to the leaching solution, and for the experiment in H_3PO_4 with the same method solution containing Pb^{2+} and Cl^{-} was used. The pH was maintained at 3 - 4 with 1M NaOH throughout the whole experiment. ICP analysis indicated that REE were removed from the HCl solution ranging from 96% to 99%, and Th >99%. Removal efficiency was even better for the H_3PO_4 solution, where all elements were removed completely (concentrations in the solution after precipitation were below the detection limit), except for Sc, whose concentration after precipitation remained at 0.02 mg/L, giving a 96% removal rate. The syntheses produced homogeneous, white crystalline powder. The crystals were spherical, smaller for the experiment with HCl than H_3PO_4 (Figure 10) and XRD (Figure 11) indicated that the synthesized products were crystalline analogue of pyromorphite. In this case no other phases were detected at the detection limit of the methods.

Table 5. Element concentrations [mg/L] in the solutions before (leaching solutions) and after co-precipitation with Pb phosphates together with the percent of removal. The uncertainty (±) is provided only where it is greater than a significant value.

	experiment D (with HCl)			experiment E (with H_3PO_4)		
Element	Before [mg/L]	After [mg/L]	Removal rate [%]	Before [mg/L]	After [mg/L]	Removal rate [%]

Sc	1.3 ± 0.09	0.01		99	0.38 ± 0.03	0.02	96
Y	19.1 ± 0.87	0.74 ± 0.03		96	18.52 ± 0.84	0.08	>99
La	35.39 ± 1.59	1.58 ± 0.07		96	12.06 ± 0.54	0.01	>99
Ce	61.98 ± 7.77	1.55 ± 0.19		97	34.09 ± 4.28	0.02	>99
Pr	5.34 ± 0.21	0.12		98	4.85 ± 0.19	b.d.	>99
Nd	17.36 ± 0.96	0.44 ± 0.02		97	8.81 ± 0.49	0.01	>99
Sm	6.79 ± 0.41	0.06		99	3.14 ± 0.19	b.d.	>99
Eu	2.05 ± 0.14	0.02		99	0.99 ± 0.07	b.d.	>99
Gd	7.83 ± 0.28	0.09		99	3.61 ± 0.13	0.01	>99
Tb	1.07 ± 0.06	0.02		98	1.12 ± 0.06	b.d.	>99
Dy	5.01 ± 0.33	0.06		99	3.29 ± 0.22	0.01	>99
Ho	1.03 ± 0.05	0.02		98	1.43 ± 0.08	b.d.	>99
Er	2.89 ± 0.18	0.05		98	1.90 ± 0.12	0.01	>99
Tm	0.42 ± 0.02	0.01		98	0.59 ± 0.02	b.d.	>99
Yb	2.69 ± 0.14	0.03		99	1.48 ± 0.08	b.d.	>99
Lu	0.44 ± 0.02	0.01		98	0.56 ± 0.03	b.d.	>99
Th	6.39 ± 0.40	0.02		>99	4.73 ± 0.29	b.d.	>99
Pb	2693.6*	5.37 ± 0.33		>99	2693.6*	0.11	>99

* calculated

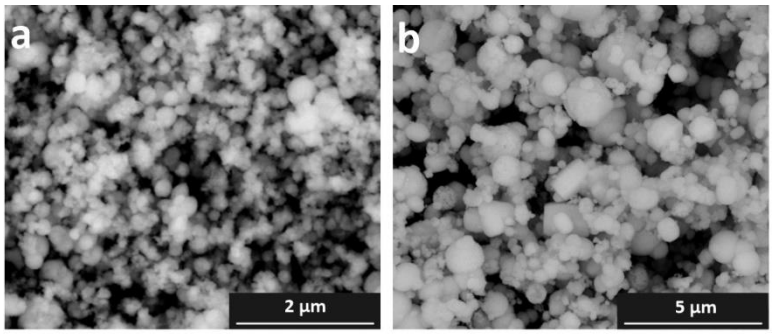

Figure 10. Backscattered electron images of REE-enriched pyromorphite precipitated in a) experiment D with HCl, and b) experiment E with H_3PO_4.

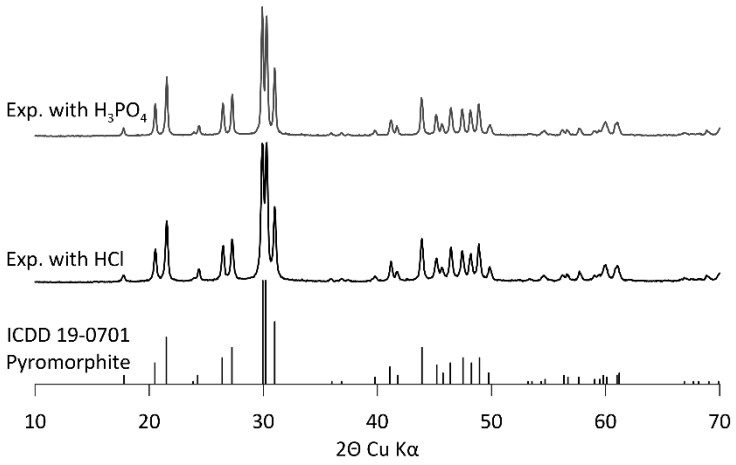

Figure 11. Diffraction patterns of pyromorphite precipitates resulting from experiment D with HCl and from experiment E with H_3PO_4.

In summary, laboratory experiments on obtaining solutions containing REE and Th by leaching from apatite and then co-precipitating REE and Th in the presence of Pb in the form of phosphates show similarly high removal efficiencies of these elements from solutions as experiments using pure laboratory reagents. Initial concentrations of REE and Th in leaching solutions ranged from tens of ppb to a few ppm. Tests conducted for two different types of leaching solutions (HCl and H_3PO_4) proved that in the co-precipitation with Pb from leaching solutions containing REE the main reaction product is REE-rich pyromorphite and the contribution of other phosphates is negligible. This indicates that co-precipitation of lead phosphates effectively removes REE and Th from solutions of various origins and is applicable in different recovery methods.

4. Conclusions

The efficiency of REE and Th removal from aqueous solutions tested for the first time by co-precipitation with Pb phosphates is very high at pH = 4 and 6. The process results in precipitation of crystalline pyromorphite (Pb5(PO4)3Cl) and other Pb-phosphate, both enriched in REE and Th. The advantage is that the process is instantaneous, proceeds at ambient temperature, and results in precipitation of heavy, crystalline sediment easy to separate by settling. The use of Pb does not raise environmental concerns because pyromorphite precipitation is a well-known method for the complete removal of Pb from solutions. The precipitate incorporates with 99- >99% efficiency all REE and Th present in the solution, as well as Pb causing neither Pb nor valuable elements are left behind. The main achievement is that this novel approach is relatively universal and can be used in the future to recover REE in any enrichment process involving leaching of minerals (e.g., apatite) or waste. The REE-Pb phosphate concentrate could be suitable for further chemical treatment to separate individual REE and Th, making the proposed process potentially usable in REE-enrichment processes.

Supplementary materials

Table S1 - Elements concentrations [mg/L] in the solutions before and after precipitation and the removal rate in the presence of Pb (exp. A, B, C) at various pH (2, 4, 6). Measurement uncertainties (±) are given only if they are greater than a significant value.

Declaration of competing interest

The authors declare that they have no known competing financial interests or personal relationships that could have appeared to influence the work reported in this paper.

Acknowledgments

The authors would like to acknowledge K. Wątor and P. Rusiniak for the ICP-OES analyses and the two anonymous reviewers who provided thoughtful comments. This research was funded by the Polish NCN grants no. 2019/35/B/ST10/03379 and 2021/43/O/ST10/01282.

References

Alves, R. C., Nascimento, M., Paulino, J. F., and Afonso, J. C., 2021. Selection of a hydrometallurgical process for rare earths extraction from a Brazilian monazite. Hydrometallurgy, 200, 105556. https://doi.org/10.1016/j.hydromet.2021.105556

Ambaye, T. G., Vaccari, M., Castro, F. D., Prasad, S., and Rtimi, S., 2020. Emerging technologies for the recovery of rare earth elements (REEs) from the end-of-life electronic wastes: a review on progress, challenges, and perspectives. Environ. Sci. Pollut. Res. , 27, 36052-36074. https://doi.org/10.1007/s11356-020-09630-2

Battsengel, A., Batnasan, A., Narankhuu, A., Haga, K., Watanabe, Y., and Shibayama, A., 2018. Recovery of light and heavy rare earth elements from apatite ore using sulphuric acid leaching, solvent extraction and precipitation. Hydrometallurgy, 179, 100-109. https://doi.org/10.1016/j.hydromet.2018.05.024

Binnemans, K., Jones, P. T., Blanpain, B., Van Gerven, T., Yang, Y., Walton, A., and Buchert, M., 2013. Recycling of rare earths: a critical review. J. Clean. Prod., 51, 1-22. https://doi.org/10.1016/j.jclepro.2012.12.037

Dang, D. H., Thompson, K. A., Ma, L., Nguyen, H. Q., Luu, S. T., Duong, M. T. N., and Kernaghan, A., 2021. Toward the circular economy of Rare Earth Elements: a review of abundance, extraction, applications, and environmental impacts. Arch. Environ. Contam. Toxicol., 81(4), 521-530. https://doi.org/10.1007/s00244-021-00867-7

Das, P., Upadhyay, S., Dubey, S., and Singh, K. K., 2021. Waste to wealth: Recovery of value-added products from steel slag. J. Environ. Chem. Eng., 9(4), 105640. https://doi.org/10.1016/j.jece.2021.105640

Du, X., and Graedel, T. E., 2011. Uncovering the global life cycles of the rare earth elements. Sci. Rep., 1(1), 145. https://doi.org/10.1038/srep00145

Dev, S., Sachan, A., Dehghani, F., Ghosh, T., Briggs, B. R., and Aggarwal, S., 2020. Mechanisms of biological recovery of rare-earth elements from industrial and electronic wastes: A review. Chem. Eng. J., 397, 124596. https://doi.org/10.1016/j.cej.2020.124596

Erust, C., Karacahan, M. K., and Uysal, T., 2022. Hydrometallurgical roadmaps and future strategies for recovery of rare earth elements. Miner. Process. Extr. Metall. Rev., 1-15. https://doi.org/10.1080/08827508.2022.2073591

EU Report, 2020. Critical Raw Materials Resilience: Charting a path towards greater Security and Sustainability. Communications (COM) 474 final.

Gaustad, G., Williams, E., and Leader, A., 2021. Rare earth metals from secondary sources: Review of potential supply from waste and byproducts. Resour Conserv Recycl, 167, 105213. https://doi.org/10.1016/j.resconrec.2020.105213

Habashi, F., 1985. The recovery of the lanthanides from phosphate rock. J. Chem. Technol. Biotechnol., 35(1), 5-14. https://doi.org/10.1002/jctb.5040350103

Henderson, P., 1984. General geochemical properties and abundances of the rare earth elements. In: Developments in geochemistry, 2, 1-32, Elsevier. https://doi.org/10.1016/B978-0-444-42148-7.50006-X

Jha, M. K., Kumari, A., Panda, R., Kumar, J. R., Yoo, K., and Lee, J. Y., 2016. Review on hydrometallurgical recovery of rare earth metals. Hydrometallurgy, 165, 2-26. https://doi.org/10.1016/j.hydromet.2016.01.035

Kasina, M., and Michalik, M., 2016. Iron metallurgy slags as a potential source of critical elements-Nb, Ta and REE. Mineralogia, 47(1-4), 15-28. https://doi.org/10.1515/mipo-2017-0004

Kumari, A., Panda, R., Jha, M. K., Kumar, J. R., and Lee, J. Y., 2015. Process development to recover rare earth metals from monazite mineral: A review. Miner. Eng., 79, 102-115. https://doi.org/10.1016/j.mineng.2015.05.003

Liu, P., Huang, R., and Tang, Y., 2019. Comprehensive understandings of rare earth element (REE) speciation in coal fly ashes and implication for REE extractability. Environ. Sci. Technol., 53(9), 5369-5377. https://doi.org/10.1021/acs.est.9b00005

Marciniak, H., Diduszko, R., Kozak, M., 2006. XRAYAN. Program do rentgenowskiej analizy fazowej, Wersja 4.0.1, KOMA, Warszawa

McLellan, B. C., Corder, G. D., Golev, A., and Ali, S. H., 2014. Sustainability of the rare earths industry. Procedia Environ. Sci., 20, 280-287. https://doi.org/10.1016/j.proenv.2014.03.035

Pan, Y., and Fleet, M. E., 2002. Compositions of the apatite-group minerals: substitution mechanisms and controlling factors. Rev Mineral Geochem, 48(1), 13-49. https://doi.org/10.2138/rmg.2002.48.2

Pålsson, B. I., Martinsson, O., Wanhainen, C., and Fredriksson, A., 2014. Unlocking rare earth elements from European apatite-iron ores. In ERES2014, 211-220.

Peiravi, M., Dehghani, F., Ackah, L., Baharlouei, A., Godbold, J., Liu, J., Manoj, M., and Ghosh, T., 2021. A review of rare-earth elements extraction with emphasis on non-conventional sources: Coal and coal byproducts, iron ore tailings, apatite, and phosphate byproducts. MINING METALL EXPLOR , 38, 1-26. https://doi.org/10.1007/s42461-020-00307-5

Pereao, O., Bode-Aluko, C., Fatoba, O., Laatikainen, K., and Petrik, L., 2018. Rare earth elements removal techniques from water/wastewater: A review. Desalin. Water Treat, 130, 71-86. doi: 10.5004/dwt.2018.22844

Ramprasad, C., Gwenzi, W., Chaukura, N., Azelee, N. I. W., Rajapaksha, A. U., Naushad, M., and Rangabhashiyam, S., 2022. Strategies and options for the sustainable recovery of rare earth elements from electrical and electronic waste. Chem. Eng. J., 135992. https://doi.org/10.1016/j.cej.2022.135992

Salo, M., Knauf, O., Mäkinen, J., Yang, X., and Koukkari, P., 2020. Integrated acid leaching and biological sulfate reduction of phosphogypsum for REE recovery. Miner. Eng., 155, 106408. https://doi.org/10.1016/j.mineng.2020.106408

Schulze, R., and Buchert, M., 2016. Estimates of global REE recycling potentials from NdFeB magnet material. Resour Conserv Recycl, 113, 12-27. https://doi.org/10.1016/j.resconrec.2016.05.004

Sethurajan, M., van Hullebusch, E.D., Fontana, D., Akcil, A., Deveci, H., Batinic, B., Leal, J.P., Gasche, T.A., Ali Kucuker, M., Kuchta, K., and Neto, I.F., 2019. Recent advances on hydrometallurgical recovery of critical and precious elements from end of life electronic wastes-a review. Crit Rev Environ Sci Technol, 49(3), 212-275. https://doi.org/10.1080/10643389.2018.1540760

Silvestri, L., Forcina, A., Silvestri, C., and Traverso, M., 2021. Circularity potential of rare earths for sustainable mobility: Recent developments, challenges and future prospects. J. Clean. Prod., 292, 126089. https://doi.org/10.1016/j.jclepro.2021.126089

Sordyl, J., Rakovan, J., Burns, P.C., Topolska, J., Włodek, A., Szymanowski, J.E.S., Sigmon, G.E., Majka, J., Manecki, M., 2023. Single crystal analysis of La-doped pyromorphite ($Pb_5(PO_4)_3Cl$). Am. Min., in press. DOI: 10.2138/am-2022-8664

Staszel, K., Jędras, A., Skalny, M., Dziewiątka, K., Urbański, K., Sordyl, J., Rybka, K., Manecki, M., submitted. Synthesis and structural investigation of new (LREE,Pb)-phosphate phases (LREE = La, Ce, Pr, Sm): Mineralogical studies for future technologies

Stone, R., 2009. As China's rare earth R&D becomes ever more rarefied, others tremble. Science 325, 1336-1337, DOI: 10.1126/science.325_1336

Stone, K., Bandara, A. M. T. S., Senanayake, G., and Jayasekera, S., 2016. Processing of rare earth phosphate concentrates: A comparative study of pre-leaching with perchloric, hydrochloric, nitric and phosphoric acids and deportment of minor/major elements. Hydrometallurgy, 163, 137-147. https://doi.org/10.1016/j.hydromet.2016.03.014

Taggart, R. K., Hower, J. C., Dwyer, G. S., and Hsu-Kim, H., 2016. Trends in the rare earth element content of US-based coal combustion fly ashes. Environ. Sci. Technol., 50(11), 5919-5926. https://doi.org/10.1021/acs.est.6b00085

Tunsu, C., Petranikova, M., Ekberg, C., and Retegan, T., 2016. A hydrometallurgical process for the recovery of rare earth elements from fluorescent lamp waste fractions. Sep. Purif. Technol., 161, 172-186. https://doi.org/10.1016/j.seppur.2016.01.048

Vahidi, E., Navarro, J., and Zhao, F., 2016. An initial life cycle assessment of rare earth oxides production from ion-adsorption clays. Resour Conserv Recycl, 113, 1-11. https://doi.org/10.1016/j.resconrec.2016.05.006

Verbaan, N., Bradley, K., Brown, J., and Mackie, S., 2015. A review of hydrometallurgical flowsheets considered in current REE projects. In: Symposium on Strategic and Critical Materials Proceedings, British Columbia Geological Survey Paper 2015-3, 147-162.

Wu, S., Wang, L., Zhao, L., Zhang, P., El-Shall, H., Moudgil, B., Huang, X., and Zhang, L., 2018. Recovery of rare earth elements from phosphate rock by hydrometallurgical processes–A critical review. Chem. Eng. J., 335, 774-800. https://doi.org/10.1016/j.cej.2017.10.143

Wu, S., Zhao, L., Wang, L., Huang, X., Zhang, Y., Feng, Z., and Cui, D., 2019. Simultaneous recovery of rare earth elements and phosphorus from phosphate rock by phosphoric acid leaching and selective precipitation: Towards green process. J. Rare Earths, 37(6), 652-658. https://doi.org/10.1016/j.jre.2018.09.012

Yang, X., Salvador, D., Makkonen, H. T., and Pakkanen, L., 2019. Phosphogypsum processing for rare earths recovery—A review. Natural Resources, 10(09), 325. 10.4236/nr.2019.109021

Zakharova, B., Komissarova, L., Traskin, V., Naumov, S., and Melnikov, P., 1996. Precipitation of rare earth phosphates from H3PO4 solutions. Phosphorus Sulfur Silicon Relat Elem, 111(1-4), 2-2.

Zimmermann, T., and Gößling-Reisemann, S., 2013. Critical materials and dissipative losses: A screening study. Sci. Total Environ., 461, 774-780. https://doi.org/10.1016/j.scitotenv.2013.05.040